

Three-body crystallization diagrams and the cooling of white dwarfs

Laurent SEGRETAIN

Centre de Recherche Astronomique de Lyon (UMR 142 du CNRS), Ecole Normale Supérieure de Lyon, 46 allée d'Italie, F-69364 Lyon Cédex 07, France

Received August 11; accepted October 16, 1995

Abstract. The 3-body crystallization diagrams of C/O/Ne ionic mixtures characteristic of white dwarf interiors are examined within the framework of the density-functional theory of freezing. The crystallization process is described more accurately than in former calculations where the three-component system was treated as an effective two-component mixture (Segretain et al. 1994). The distillation process due to neon-crystallization is found to occur only for the late stages of crystallization. At the beginning, the presence of neon plays only a minor role and the phase diagram resembles a pure carbon-oxygen diagram. The final phase diagram is found to exhibit an azeotropic point with a neon concentration $x_{Ne} = 0.22$, a carbon concentration $x_C = 0.78$ and an oxygen concentration $x_O = 0$, so that during the distillation process, the fluid crystallizes into a pure neon-carbon solid. The critical temperature is $T_A = 0.85 T_C$, where T_C is the pure carbon crystallization temperature. We use this accurate phase diagram to calculate the total gravitational energy released during white dwarf crystallization and the related time delay. The final result yields $\Delta\tau \approx 2.6$ Gyr, among which about 20% are due to the neon-distillation process.

Key words: dense matter – phase diagrams – white dwarfs

to examine in details the effect of these different crystallization processes, Segretain & Chabrier (1993) have calculated the crystallization diagrams of dense *binary* ionic mixtures with arbitrary charge ratios under thermodynamic conditions characteristic of dense stellar plasmas. The diagram was found to evolve from a spindle form to an azeotropic, and eventually an eutectic form, with increasing charge ratio Z_2/Z_1 . These binary diagrams have been used by Segretain et al. (1994) to compute the cooling of a C/O/Ne/Fe WD. The crystallization processes were shown to bear major consequences on the cooling time and the luminosity function of old WDs (Segretain et al. 1994; Hernanz et al. 1994). In these calculations, and given the complexity of the calculation of multi-component phase diagrams, the ternary C/O/Ne or C/O/Fe mixtures were assumed to behave as *effective binary* mixtures composed of neon (resp. iron) and an element of average charge $\langle Z \rangle = 7$. The calculations showed that neon plays a major role in the cooling of WD, because of a distillation process bound to the presence of an azeotropic point in the phase diagram. The resulting sedimentation of neon was found to have an effect on the cooling time comparable to the one due to the crystallization of the carbon-oxygen mixture itself. In this paper we have extended the calculations of Segretain & Chabrier (1993) to the calculation of a true *ternary* C/O/Ne diagram. The diagram is calculated within the framework of modern density functional theory (DFT) of freezing, and the plasma correlation functions are calculated within the mean spherical approximation (MSA) (see Segretain & Chabrier 1993 for details). In Sect. 3, we describe the resulting diagram and we compare it with the previous effective two-body diagram. In Sect. 4, we use this ternary phase diagram to derive the global effect of neon crystallization on the cooling of a WD.

2. Method

The crystallization diagram has been computed within the framework of the density functional theory (DFT) of freez-

1. Introduction

Following the pioneer work of Stevenson (1980), Garcia-Berro et al. (1988) have demonstrated the importance of the shape of the crystallization diagram on the cooling history of white dwarfs (WD). In the eighties, all the work has focussed on the crystallization of a pure carbon-oxygen mixture (Stevenson 1980; Mochkovitch 1983; Barrat et al. 1988; Ichimaru et al. 1988). More recently, Isern et al. (1991) have pointed out the importance of minor elements, in particular neon, on the general cooling process. In order

ing. One of the main advantages of the DFT is that we can calculate directly the free energy *difference* between the solid and the fluid phases. We consider a mixture of N_i ions of charge Z_i ($i = 1, 2, 3$) in a volume V at a temperature T . The number densities and molar fractions read respectively $\rho_i = N_i/V$ and $x_i = N_i/N$ ($i=1,2,3$) with $N = \sum_i N_i$. The electronic and ionic coupling parameters are defined respectively as $\Gamma_e = e^2/a_e k_B T$ and $\Gamma_i = Z_i^{5/3} \Gamma_e$, where $a_e = (4\pi/3 N_e/V)^{-1/3}$ is the mean inter-electronic distance and $\langle Z \rangle = \sum_i x_i Z_i$ is the average charge. The free energy of the liquid phase reads:

$$F_L = \sum_{i=1}^3 x_i \left(\ln x_i \frac{Z_i}{\langle Z \rangle} + F^{OCP}(\Gamma_i) \right) \quad (1)$$

where the first term on the r.h.s. is the ideal ionic contribution whereas the second term denotes the correlation terms. This term is well approximated by a linear interpolation of the free energies of the pure phases (designated by the superscript OCP -One Component Plasma-), for which analytical fits are available (Stringfellow et al. 1990). The free energy of the solid writes:

$$F_S = F_L + \Delta F$$

$$\Delta F = \Delta F^{id} + \Delta F^{ex}$$

with

$$\frac{\Delta F^{id}}{NkT} = \sum_{\nu=1}^3 \frac{\rho_{\nu S}}{\rho_L} \left\{ \ln \left[\frac{(\alpha_\nu/\pi)^{3/2} \rho_{\nu S}}{\rho_{\nu L} \rho_S} \right] - \frac{3}{2} \right\} \quad (2)$$

and

$$\frac{\Delta F^{ex}}{NkT} = -\frac{1}{2} \sum_G \sum_{\nu, \mu=1}^3 \frac{\rho_{\nu S} \rho_{\mu L}}{\rho_L^2} C_{\nu\mu}(\mathbf{G}) \times \exp \left[-\frac{G^2}{4} \left(\frac{1}{\alpha_\nu} + \frac{1}{\alpha_\mu} \right) \right] \quad (3)$$

where \sum'_G represents the sum over all the reciprocal lattice vectors (RLV) for $\mathbf{G} \neq 0$. The ρ_ν denote the number density of the ν component either in the solid (S) or in the liquid phase (L). For each concentration x_ν at a given temperature T , ΔF is minimized with respect to the width of the gaussians α_ν in order to calculate F_S . The $C_{\mu\nu}(\mathbf{G})$ are the Fourier transforms of the direct correlation functions of the liquid near crystallization. These latter are computed within the framework of the Mean Spherical Approximation (MSA). As in Segretain & Chabrier (1993), we use a reduction of the second RLV in $C_{\mu\nu}(\mathbf{G})$ in order to obtain a bcc crystal for the one component system at $\Gamma_e Z^{5/3} = 178$ (Slattery et al. 1982; Stringfellow et al. 1990).

3. C/O/Ne phase diagram

Since the pressure of the degenerate electron gas is considerably larger than the ionic pressure under the conditions of interest (degenerate stars interiors), fluid-solid phase equilibrium at constant pressure and temperature is equivalent to phase coexistence at constant electron density ρ_e and temperature T , i.e. at constant Γ_e . For fixed values of Γ_e and T , the concentrations of coexistent fluid and disordered solid phases are determined by usual double-tangent constructions.

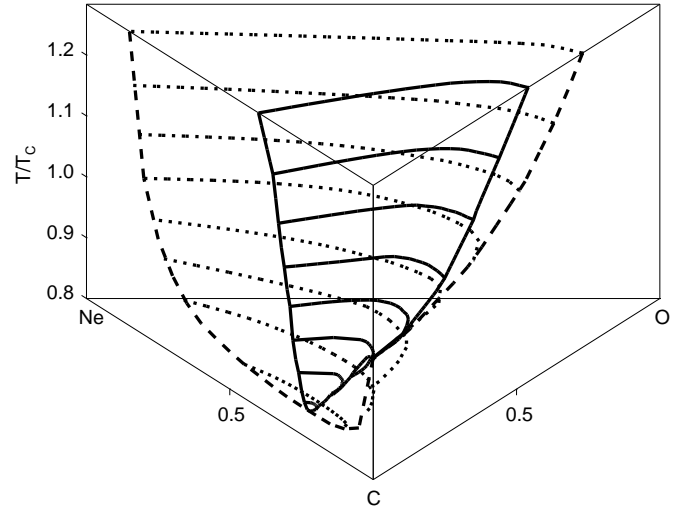


Fig. 1. C/O/Ne crystallization diagram for $\Gamma_e \geq 7$. The coordinates of the azeotropic point are $T_a = 0.85 T_C$ and $x_C = 0.78$, $x_O = 0.0$, $x_{Ne} = 0.22$, where T_C is the crystallization temperature of pure carbon. The bold solid lines visualize the *liquidus* and the bold dotted and dashed lines the *solidus*.

Figure 1 shows the resulting 3-component phase diagram for the C/O/Ne mixture under thermodynamic conditions characteristic of WD interiors, i.e. $10^{10} \leq P \leq 10^{16}$ Mbar, $10^3 \leq \rho \leq 10^6$ gcm $^{-3}$ and for $T \leq 5.10^7$ K, which yields $\Gamma_e \geq 7$. The 3-D picture of the C/O/Ne diagram can be first visualized with the 2-D projections on the C/O, C/Ne and O/Ne planes. Note that, for sake of clarity, only the lower part of the general diagram ($T/T_C \leq 1.2$, where T_C is the crystallization temperature of pure carbon), is shown. The pure carbon and oxygen mixture ($X_{Ne} = 0$) limit crystallize into a spindle diagram, as expected from the small charge ratio. So does the bare O/Ne mixture ($X_C = 0$ limit), with a larger crystallization temperature, since $T_{Ne} > T_C$ and $T_O > T_C$ where T_i , $i = C, O, Ne$, denotes the crystallization temperature of pure carbon, oxygen and neon respectively. The pure C/Ne ($X_O = 0$) diagram exhibits an azeotropic behavior with an azeotropic point for $x_C = 0.78$, $x_{Ne} = 0.22$ and $T_a = 0.85 T_C$. The true 3-body diagram is visualized by the bold lines, where the solid line display the

liquidus and the dotted and dashed lines represent the *solidus*. As shown, the azeotropic point of the *three*-body diagram is the azeotropic point of the *two*-body C/Ne mixture ($X_O = 0$), which is the lowest stable point for the liquid in the three-component C/O/Ne mixture.

We also note that, for small concentrations of neon, and for temperatures well above the azeotropic temperature, the liquid and the solid have the same Ne-concentration. The mixture then crystallizes like an equivalent Ne-enriched C/O mixture. In other words, at high temperature, and for low concentrations of neon, the crystallization diagram is not affected by the presence of neon. As the temperature approaches the azeotropic temperature, neon starts to modify the crystallization process. The distillation process, as described in Segretain et al. (1994), begins. The liquid becomes enriched in neon and the diagram evolves into the azeotropic shape.

This behavior is different from the one obtained with the *effective* 2-body mixture used in Segretain et al. (1994), where the Ne-enriched process was found to start as soon as crystallization set in. As described above, the present complete 3-body calculations show that C/O crystallization first takes place without Ne-enrichment.

This bears important consequences for the astrophysical application, as will be shown in the next section, where the diagram will be examined for C/O/Ne concentrations characteristic of WD interiors.

4. Consequences on white dwarf cooling

The mass fractions characteristic of WD interior are $X_{Ne} = 1.0\%$ and $X_C = X_O = 49.5\%$, uniformly distributed in the liquid phase (the effect of an initial non-uniform profile has been examined in details in Segretain et al. 1994). The exact C/O mass fraction in WD interiors is subject to important uncertainties. The present equimolar distribution has been chosen for the sake of simplicity. Larger initial oxygen concentrations in the core of the WD will, at any rate, lead to even smaller energy release by Neon sedimentation. As shown on the diagram of Fig. 1, the process of crystallization develops as follows. Crystallization begins at the center of the star where the density, and thus the crystallization temperature, is the largest ($T_C \propto \rho^{1/3}/178$). In that case, as mentioned in the previous section, we get the same behaviour as for a pure C/O mixture, but with concentrations $X_C = X_O = 0.495$, i.e the same neon concentration in the solid and the liquid phase. Until $T/T_C = 1.12$ (point A in Fig. 2) the resulting sedimentation of oxygen is the same as in a pure C/O WD. Beyond $T/T_C = 1.12$, the distillation process begins, so that neon concentration becomes different in the two phases. However, the neon effect on the release of gravitational energy will be small because, at point A, about 70% (in mass) of the star has already crystallized. This is very different from the result obtained with the *effective* 2-body diagram, where neon was found to crystallize first.

At the end of the distillation process, i.e. at the azeotropic temperature (point B in Fig. 2), all neon has crystallized; the remaining liquid contains only carbon and oxygen and sedimentation of oxygen continues normally. The oxygen and neon profiles in solid along the crystallization process are shown on Fig 2.

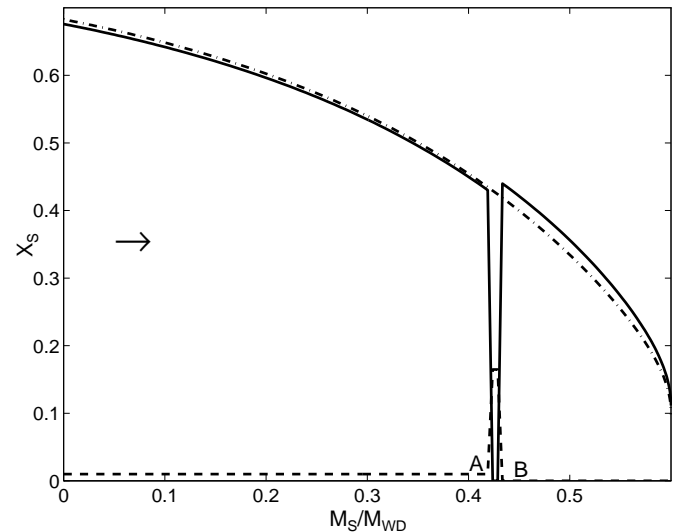


Fig. 2. Concentration profiles at the end of the crystallization, for two different WDs. Dot-dashed line : oxygen profile for a pure C/O WD. Solid line : oxygen profile for a C/O/Ne WD. Dashed line : neon profile for a C/O/Ne WD. The crystallization front evolves as indicated by the arrow. The neon-distillation process begins at point A and ends at point B. During this process, the solid which forms does not contain oxygen, since the azeotropic point is characterized by $X_O = 0$. After point B, all neon has crystallized; the remaining solid contains only carbon and oxygen, and the usual oxygen sedimentation process proceeds again.

These concentration profiles are used to compute the evolution of the binding energy along crystallization, as in Segretain et al. (1994). The difference of binding energy due to crystallization is $\Delta B = 3.10 \cdot 10^{46}$ erg, only $\sim 20\%$ more than the one obtained for the crystallization of a pure C/O WD. The effect of neon crystallization, when properly taken into account, is then smaller than when treated within the effective 2-body approximation. The release of binding energy due to the crystallization of the C/O/Ne mixture yields a total time delay about 20% larger than the one due to the crystallization of a pure C/O mixture, i.e $\Delta\tau \approx 2.6$ Gyr. The effect intrinsically due to neon crystallization is about 0.4 Gyr. This effect on the cooling time, however, does not modify the age of the Galactic disk, based on the calculation of the WD luminosity function, obtained by Hernanz et al. (1994), as explain in section 3.2 of the paper of Hernanz et al. (1994).

5. Conclusion

In this paper we have computed for the first time the crystallization diagram of a *three-component* C/O/Ne mixture characteristic of WD interiors. The general phase diagram is found to be of the azeotropic form. We use this phase diagram to compute the crystallization process of a uniform distribution C/O/Ne WD with $X_{Ne} = 1.0\%$ and $X_C = X_O = 49.5\%$. The presence of neon is found to be inconsequential at the beginning of the crystallization process. The neon concentration remains the same in the solid and in the liquid phase, so that the major process is the sedimentation of oxygen, characterized by a spindle diagram, as found for a pure C/O WD. When 70% (in mass) of the WD has crystallized, the shape of the diagram evolves substantially, and the influence of neon becomes important. A distillation process begins and all the neon left in the liquid crystallizes at the azeotropic concentration/temperature, i.e $T_a = 0.85 T_C$, $x_C = 0.78$, $x_O = 0.0$ and $x_{Ne} = 0.22$. This crystallization process is different from the one obtained with the *effective 2-body* diagram for which the distillation process is found to begin as soon as crystallization sets in. The time delay produced by the afore-mentioned general crystallization process is about 2.6 Gyr, i.e about 20% larger than the one obtained for a pure C/O mixture. The effect of neon is only of 0.4 Gyr. These detailed calculations show that, though not completely negligible, the effect of neon, and iron as well, does not bear important consequences on the general cooling history of WDs.

Acknowledgements. The author are grateful to G. Chabrier for helpful discussions.

References

- Barrat, J.L., Hansen, J.P., Mochkovitch, R. 1988. A&A, 199, L15.
- Garcia-Berro, E, Hernanz, M., Mochkovitch, R., Isern, J. 1988. A&A, 193, 141.
- Hernanz, M., Garcia-Berro, E., Isern, J., Mochkovitch, R., Segretain, L., Chabrier, G. 1994. ApJ, 434, 652.
- Ichimaru, S., Iyetomi, H., Ogata, S. 1988. ApJ, 334, L17.
- Isern, J., Mochkovitch, R., Garcia-Berro, E., Hernanz, M. 1991. A&A, 241, L29.
- Mochkovitch, R. 1983. A&A, 122, 212.
- Segretain, L., Chabrier, G. 1993. A&A, 271, L13.
- Segretain, L., Chabrier, G., Hernanz, M., Garcia-Berro, E., Isern, J., Mochkovitch, R. 1994. ApJ, 434, 641.
- Slaterry, W.L., Doolen, G.D., DeWitt, H.E. 1982. Phys. Rev. A, 26, 2255.
- Stevenson, D.J. 1980. Journal de Physique, 41 C2, 61.
- Stringfellow, G.S., DeWitt, H.E., Slaterry, W.L. 1990. Phys. Rev. A, 41, 1105.